Statistical Analysis of Dark Current in Silicon Photomultipliers

Giuseppina Valvo, Alfio Russo, Delfo Sanfilippo,
Giovanni Condorelli, Clarice Di Martino,
Beatrice Carbone, PierGiorgio Fallica
IMS-R&D STMicroelectronics, stradale Primosole, 50
95121 Catania, ITALY
giusy.valvo@st.com

Roberto Pagano, Sebania Libertino,
Salvatore Lombardo
CNR-IMM, Ottava Strada Zona Industriale, 5, 95121
Catania, ITALY
salvatore.lombardo@imm.cnr.it

***Abstract*—The aim of this paper is to investigate on a statistical basis at the wafer level the relationship existing among the dark currents of the single pixel compared to the whole Silicon Photomultiplier array. This is the first time to our knowledge that such a comparison is made, crucial to pass this new technology to the semiconductor manufacturing standards. In particular, emission microscopy measurements and current measurements allowed us to conclude that optical trenches strongly improve the device performances.**

Keywords - silicon photomultipliers; dark current; wafer level.

I. INTRODUCTION

Silicon-based single photon detectors [1-11] have been widely investigated since their appearance thanks to their interesting features: reduced dimensions, low weight, low fabrication costs, insensitivity to magnetic fields, and low operation voltage. Starting from single diode devices, progress in the field has driven the microelectronic industry to go towards designing and fabricating arrays of such devices, that is, avalanche detectors with an integrated quenching resistor connected in parallel and operating in Geiger mode, referred to as Si Photomultipliers (SiPMs), to cover areas up to ≈10 mm^2 per device. The principle of operation of each single avalanche detector consists in a p-n junction biased above the breakdown voltage (BV). Thanks to the high quality substrate and fabrication technology (low defect concentration), it can remain quiescent above the BV until a photon is absorbed in the depletion volume. Once the photon is absorbed, the electron-hole (e-h) pair generated triggers a self-sustaining avalanche breakdown. The avalanche is switched off through an opportunely designed quenching resistance that reduces the voltage below breakdown as soon as the current flows through the diode. The operation of the whole SiPM array is the parallel sum of the currents produced by each single pixel.

Aim of this paper is to investigate on a statistical basis at the wafer level the relationship existing among the dark currents of the single pixel compared to the whole SiPM array. This is the first time to our knowledge that such a comparison is made, crucial to pass this new technology to the semiconductor manufacturing standards.

II. EXPERIMENTAL

Single cells and arrays of 64x64 cells were fabricated in B doped Si wafers An enrichment region was obtained through B implantation, to define both the device active area and the BV. The cathode was fabricated through diffusion from a heavily doped polysilicon layer [12]. The quenching resistor was integrated on the cathode of the cell itself and fabricated using low-doped polysilicon. Finally, optical trenches surround the pixel active area in order to reduce electro-optical coupling effects (crosstalk) between adjacent microcells. A schematic cross-section of the final structure of the single cell is shown in Figure 1.

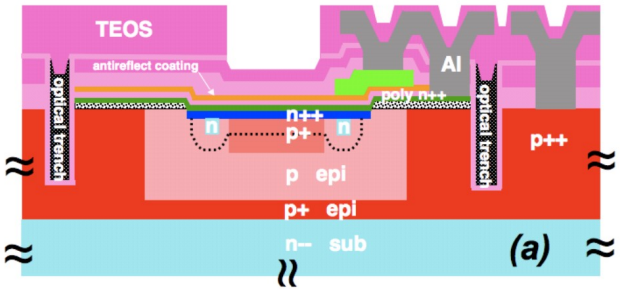

Figure 1. Schematic cross section of the SiPM single pixel, showing the central active area with the cathode (indicated as "n++"), the enriched anode ("p+"), the sub-anode ("p epi"), the anode contact region ("p+ epi"), the substrate ("n-- sub"), and the optical trenches.

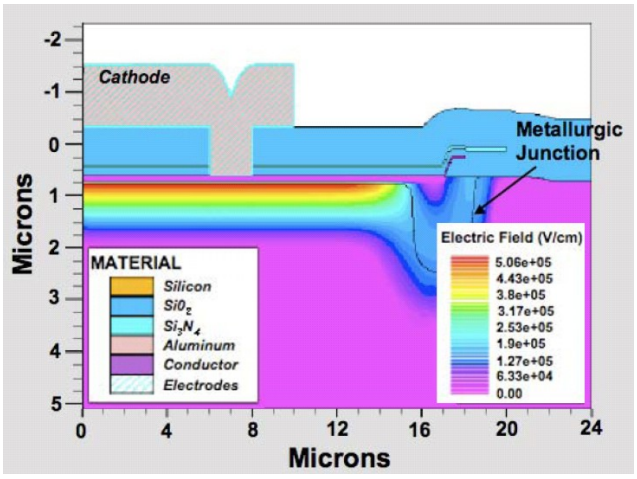

Figure 2. 2D TCAD simulation of the electric profile performed at a bias polarization of -30 V in the structure sketched in Fig. 1.

Copyright (c) IARIA, 2011. ISBN: 978-1-61208-145-8

Figure 2 shows the 2D simulation of the electric profile performed at a bias polarization of -30 V. The electric field at the lateral border is well below its maximum value for junction breakdown and is negligible with respect to the maximum value in the active region, in which, on the contrary, the field is above the critical field for avalanche breakdown.

Devices basic electrical characterization provided a breakdown voltage in agreement with that predicted by TCAD simulation, and equal to about -28.0V at room temperature.

Emission microscopy (Em.Mi) measurements were carried out at 25°C using an overvoltage (*i.e.*, voltages above the junction breakdown voltage, ΔV) of 3V.

III. RESULTS AND DISCUSSION

One of the major issues to solve is the minimization of the cross-talk effect among close pixels. An improper isolation scheme results in an avalanche correlation effect which trigger avalanches in close pixels (Fig. 3(a)). The avalanches in close pixels are likely triggered either by photons or by minority carriers produced by the avalanche of a primary pixel which migrates to close pixels causing new avalanches. The use of a proper electro / optical isolation trench scheme dramatically improves the situation (Fig. 3(b)), rendering negligible the cross-talk effect among neighbor pixels, and strongly reducing the dark current (from 300 to 10 μA).

The relationship among the dark currents in single pixels and in complete SiPM arrays is investigated in Fig. 4. We model the dark current of a single pixel as [13]:

$$I_D = q\left(\frac{N_{Def}}{\tau} + \frac{A_{Pixel}}{\tau_i}\right)G \qquad (1)$$

where q is the elementary charge, N_{Def} the number of carrier generating defects per pixel in the active volume, τ the average time for carrier generation event by one defect, A_{Pixel} the single pixel active area, τ_i the average time per unit area for the intrinsic carrier generation due to diffusion from the quasi neutral regions to the active volume, and G the gain, *i.e.*, the total number of carriers generated in a single avalanche, from the avalanche buildup to the avalance quenching and pixel recharge. We find that the I_D of the overall SiPM devices is simply the sum of the currents of single pixels as above modeled, with no contribution of extrinsic defects providing high leakage paths. In particular Fig. 4 shows frequency histograms comparing the dark currents measured at room temperature of single pixels and SiPM arrays for a total of 952 devices at overvoltages (*i.e.,* voltages above the junction breakdown voltage) of 2, 3, and 4 V. The SiPM device contains 4096 pixel, so the respective currents of SiPM to single pixel should stay in ratio of about 4,000, as actually found.

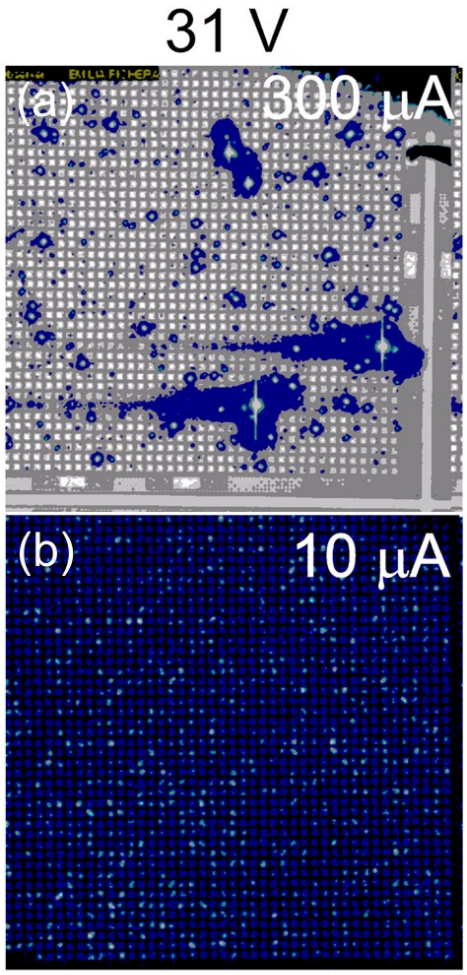

Figure 3. Emission Microscopy measurements on SiPM arrays (a) without and (b) with optical trenches.

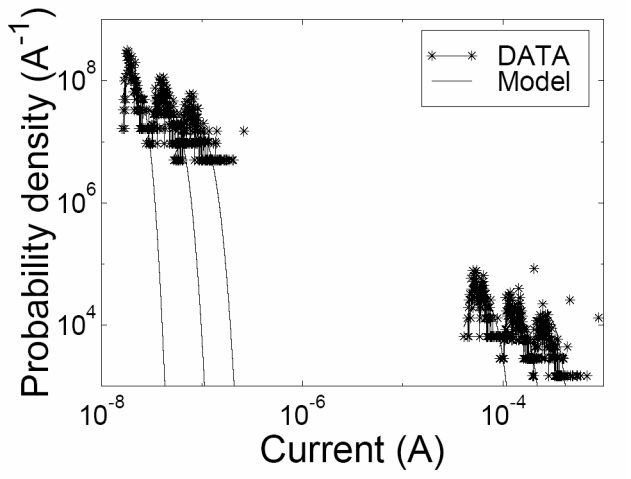

Figure 4. Probability density as a function of the output current at overvoltages of 2V, 3V and 4V, for both single pixels and arrays (having 4096 cells). The solid red lines are the model results.

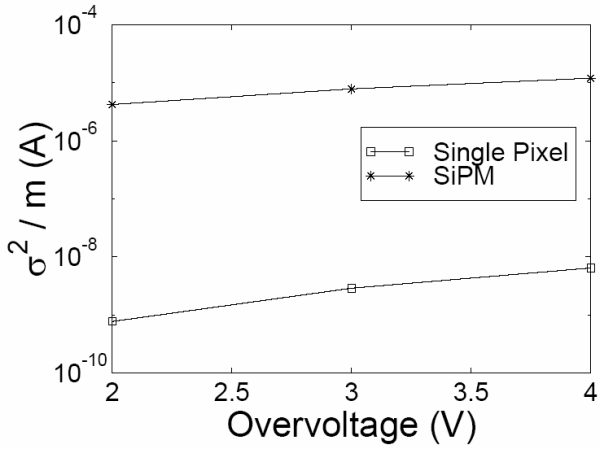

Figure 5. Experimental values of the variance divided by average device current as a function of the device overvoltage for the single pixel (in blue) and the SiPM (in red)

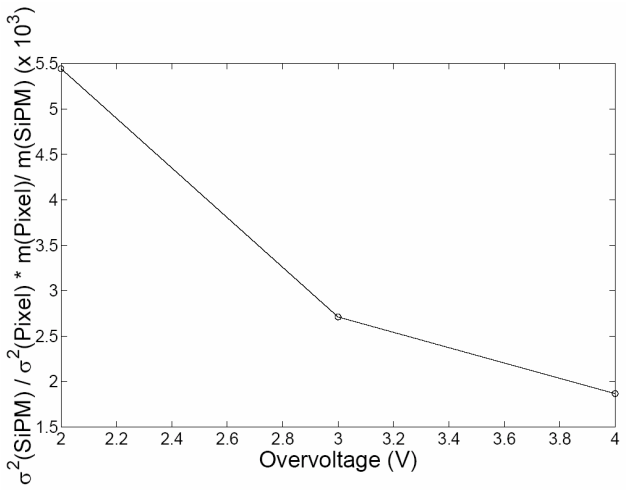

Figure 6. Experimental values of the ratio of the variance divided by the average device current between SiPMs and single pixels as a function of the overvoltage. The model, in good agreement with the experimental results, predicts that the ratio should be equal to the number of pixels in the SiPM device, equal to 4,096.

To model I_D in the present devices, we note that at room temperature the term $\frac{N_{Def}}{\tau}$ dominates, so the I_D statistics should essentially coicide with the N_{Def} statistics. The prevalence of the $\frac{N_{Def}}{\tau}$ term has been demonstrated through the temperature dependence of the leakage current, as reported in ref. [14]. For the N_{Def} statistics we assume the Poisson statistics so we find that the probability dP of having a dark count between I_D and I_D+dI_D is:

$$\frac{dP}{dI_D} = N \exp\left[\frac{m_{I_D}}{\sigma^2_{I_D}}\left(I_D \log(m_{I_D}/I_D) + (I_D - m_{I_D})\right)\right] \quad (2)$$

where N is a normalization constant, m_{I_D} is the statistical average of the dark current and $\sigma^2_{I_D}$ is the variance. In the case of the SiPM arrays the same expression holds. Fig. 4 reports also the model curves, which show a good match with the experimental data. The model predicts that the combination of statistical parameters $\frac{\sigma^2_{I_D}}{m_{I_D}}$ should be equal to $\frac{q}{\tau}G$ or $4096 \times \frac{q}{\tau}G$, for the single pixel and the SiPM array, respectively. Fig. 5 reports the experimental values of $\frac{\sigma^2_{I_D}}{m_{I_D}}$ as a function of the device overvoltage. As the overvoltage increases, $\frac{\sigma^2_{I_D}}{m_{I_D}}$ grows, due to the G increment. Morevover the ratio of $\frac{\sigma^2_{I_D}}{m_{I_D}}$ between SiPM and single pixel results of the order of 4,000 (Fig. 6), as predicted by the model. More details will be shown in the presentation.

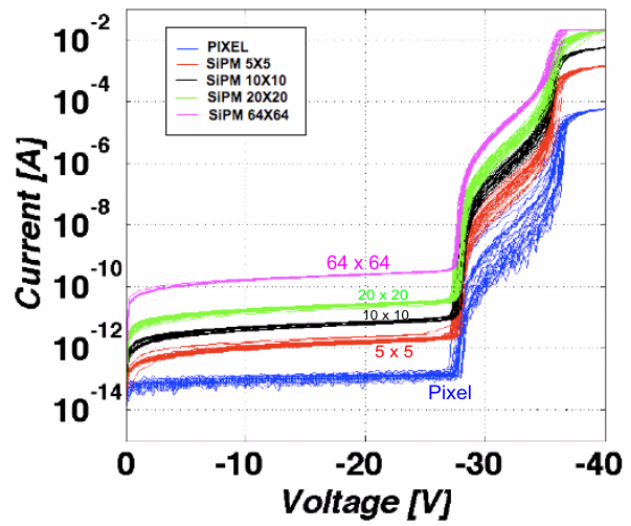

Figure 7. Reverse current for single pixels and arrays from 25 up to 4096 cells.

Further developments are ongoing and will be reported at the conference. In particular we would like to mention that an improved version of our SiPM technology shows a further reduced dark current leakage (Fig. 7). This is

Copyright (c) IARIA, 2011. ISBN: 978-1-61208-145-8

attributed to an improved minority carrier lifetime (larger τ_i in Eq. (1)), obtained through a better device architecture [14].

ACKNOWLEDGMENTS

CNR authors gratefully acknowledge ST support for research funding.

REFERENCES

[1] R.H. Haitz, "Model for the electrical behavior of a microplasma", J. Appl. Phys., 35 (1964), p. 1370.

[2] R. H. Haitz, "Mechanisms contributing to the noise pulse rate of avalanche diodes," J. Appl. Phys., 36, (1965), pp. 3123–3131

[3] R. J. McIntyre, "The distribution of gains in uniformly multiplying avalanche photodiodes: Theory," IEEE Trans. Electron Devices, 19, 6, (1972), pp. 703–713.

[4] "SPCM-AQR Data Sheet", Perkin Elmer Optoelectronics, available online http://www.htds.fr/doc/optronique/scientifiqueBiomedical/SPCM-AQR.pdf

[5] S. Cova et al., "Active-quenching and gating circuits for single-photon avalanche diodes (SPADs)", IEEE Trans. Nucl. Sci., 29, 1, (1982), pp. 599–601.

[6] F. Zappa et al., "Fully-integrated active-quenching circuit for single-photon detection", Proc. of the 28th European Solid-State Circuits Conference, ESSCIRC 2002, p. 355.

[7] S. Vasile et al., "High gain avalanche photodiode arrays for DIRC applications", IEEE Trans. Nucl. Sci. 46 (1999) p. 848.

[8] P. P. Antich, "Avalanche photo diode with local negative feedback sensitive to UV, blue and green light", Nucl. Instrum. Meth. A, 389 (1997) pp. 491-498.

[9] G. Bondarenko, "Limited Geiger-mode microcell silicon photodiode: new results", Nucl. Instrum. Meth. A, 442 (2000) pp. 187-192.

[10] V. Golovin, Avalanche Photodetector, Russian Agency for Patents and Trademarks, Patent No. RU 2142175 (1998).

[11] Z. Sadygov, Avalanche Detector, Russian Agency for Patents and Trademarks, Patent No. RU 2102820 (1998).

[12] E. Sciacca et al., "Silicon Planar Technology for Single-Photon Optical Detector", IEEE Trans. Electr. Dev.,50, 4 (2003) pp. 918-925.

[13] R. Pagano, S. Lombardo, S. Libertino, G.Valvo, G. Condorelli, B. Carbone, D. N. Sanfilippo, and G. Fallica, "Understanding dark current in pixels of silicon photomultipliers", IEEE, Proc. Of 40th European Solid State Device Research Conference, pp. 265-268 (2010)

[14] R. Pagano, S. Libertino, D. Corso, G. Valvo, D. Sanfilippo, G. Fallica, and S. Lombardo, "Dark current in SiPM pixels: data and model", article in preparation.

Copyright (c) IARIA, 2011. ISBN: 978-1-61208-145-8